Statistical theory of interior-exterior transition and collision probabilities for minor bodies in the solar system

Shane Ross
Control and Dynamical Systems
California Institute of Technology
MC 107-81, Pasadena, CA 91125, USA
shane@cds.caltech.edu

Abstract

The dynamics of comets and other solar system objects which have a three-body energy close to that of the collinear libration points are known to exhibit a complicated array of behaviors such as transition between the interior and exterior Hill's regions, temporary capture, and collision. The invariant manifold structures of the collinear libration points for the planar, circular restricted three-body problem, which exist for a range of energies, provide the framework for understanding these complex dynamical phenomena from a geometric point of view. The stable and unstable invariant manifold tubes associated to libration point orbits are the phase space structures that provide a conduit for particles travelling to and from the secondary body (e.g., Jupiter). Using the structures around libration points, a statistical theory of the probability of interior-exterior transition and the probability of collision with the secondary body can be developed. Comparisons with observations of Jupiter family comets are made.

Introduction

Several Jupiter-family comets such as P/Oterma, P/Gehrels 3, and P/Helin-Roman-Crockett make a transition from heliocentric orbits inside the orbit of Jupiter to heliocentric orbits outside the orbit of Jupiter and vice versa (Carusi, Kresák, Pozzi, and Valsecchi [1985] and Koon, Lo, Marsden, and Ross [2001]). During this transition, the comet can be captured temporarily by Jupiter for one to several orbits around Jupiter (Tancredi, Lindgren, and Rickman [1990], and Howell, Marchand, and Lo [2000]). The Tisserand parameters of these objects, termed the *quasi-Hildas* (hereafter QHs) by Kresák [1979], are slightly in excess of 3. The possible pre-capture orbital history of D/Shoemaker-Levy 9 (henceforth referred to as SL9) also places it within this group (Benner and McKinnon [1995]).

An important feature of the motion of these comets is that during the phase right before and after their encounter with Jupiter, their orbits pass close to the libration points L_1 and L_2 of the sun-Jupiter system. This has been pointed out by many authors, including Tancredi, Lindgren, and Rickman [1990], Valsecchi [1992], and Belbruno and Marsden [1997]. Hence objects with low velocity relative to these points (i.e., orbits with apoapse near L_2 or periapse near L_1) are most likely to be captured (Kary and Dones [1996]).

During the short time just before an encounter with Jupiter, the most important orbital perurbations are due to Jupiter alone, as suggested by the passages of comets by L_1 and L_2. N-body effects of Saturn and the other large

planets surely play a significant role over significantly longer times, but we concentrate here on the time right before a comet's encounter with Jupiter. To simplify the analysis, we use the most rudimentary dynamical model, namely, the circular, planar restricted three-body model (PCR3BP), to determine the basic phase space structure which causes the dynamical behavior of the QH comets. Furthermore, since the PCR3BP is an adequate starting model for many other systems, results can be applied to other phenomena in the solar system, such as the near-Earth asteroid (NEA) problem, wherein one considers the motion of an asteroid on an energy surface in the sun-Earth system where libration point dynamics are important.

Lo and Ross [1997] suggested that studying the L_1 and L_2 invariant manifold structures would be a good starting point for understanding the capture and transition of these comets. Koon, Lo, Marsden, and Ross [2000] studied the stable and unstable invariant manifolds associated to L_1 and L_2 periodic orbits. They took the view that these manifolds, which are topologically tubes within an energy surface, are phase space conduits transporting material to and from Jupiter and between the interior and exterior of Jupiter's orbit.

In the present paper, we wish to extend the results of Koon, Lo, Marsden, and Ross [2000] to obtain *statistical* results. In particular, we wish to address two basic questions about QHs and NEAs: How likely is a QH collision with Jupiter or a NEA collison with Earth? How likely is a P/Oterma-like interior-exterior resonance transition? With this work, we put SL9, NEA impacts, and interior-exterior transitions into the broader context of generic motion in the restricted three-body problem.

The paper is broken up into two sections. In section 1, we discuss some phenomena of the QH comets, namely interior-exterior and collisions with Jupiter. In section 2, we frame the above questions as a transport problem, viewing the PCR3BP as the underlying dynamical system. We also summarize the results and suggest future directions.

1 The Quasi-Hilda Group of Comets

The QH group of comets is a small group of strongly Jupiter-interacting comets having a Tisserand parameter slightly above 3, characterized by repeated and long-lasting temporary captures (Benner and McKinnon [1995]). As authors have noted, the capture process frequently moves bodies from orbits outside Jupiter's orbit to inside Jupiter's orbit, passing by L_1 and L_2 in the process of approaching or departing from Jupiter's vicinity (e.g., Kary and Dones [1996]). We will refer to this type of transition as an *interior-exterior* transition.

Interior-Exterior Transition. In Figure 1(a), we show the interior-exterior transition of QH P/Oterma in a sun-centered inertial frame. The interior orbit is in an exact 3:2 mean motion resonance with Jupiter* while the exterior orbit is near the 2:3 resonance with Jupiter. In Figure 1(b), we show a homoclinic-heteroclinic chain of orbits in the PCR3BP as seen in the rotating frame. This is a set of orbits on the intersection of L_1 and L_2 stable and unstable manifolds with energies equal to that of P/Oterma. The homoclinic-heteroclinic chain

*By *exact*, we mean that P/Oterma orbits the sun three times while Jupiter orbits the sun twice, as seen in an inertial frame.

is believed to form the backbone for temporary capture and interior-exterior transition of QHs, as can be seen when the orbit of P/Oterma in the rotating frame is overlayed as in Figure 1(c) (Koon, Lo, Marsden, and Ross [2000]).

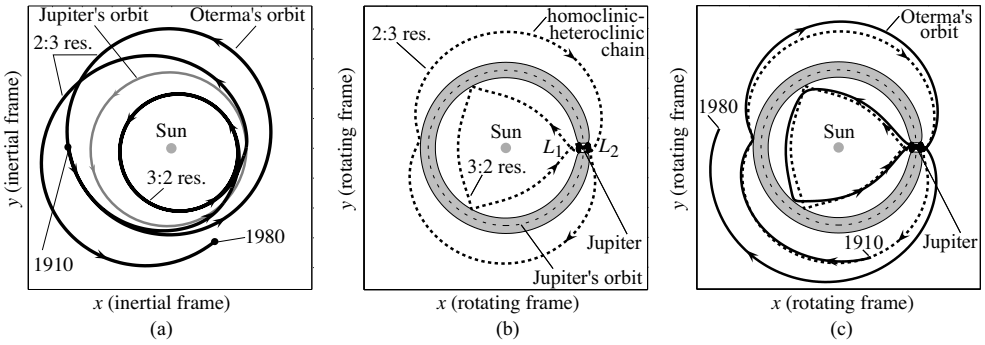

Figure 1: (a) Orbit of quasi-Hilda comet P/Oterma in sun-centered inertial frame during time interval AD 1910–1980 (ecliptic projection). (b) A homoclinic-heteroclinic chain for the energy of P/Oterma in the circular, planar restricted three-body problem, as seen in the rotating frame with the sun and Jupiter fixed. (c) The orbit of P/Oterma, transformed into the rotating frame, overlaying the chain.

Collision with Jupiter. At the time of its discovery, SL9 was only 0.3 AU from Jupiter and broken up into several fragments due to tidal disruption on an earlier approach within the planet's Roche limit (Marsden [1993]). Integrations indicated that it would collide with the planet (Chodas and Yeomans [1993]), which it subsequently did in July 1994.

Likely Pre-Collision Heliocentric Orbit of SL9. Pre-collision integrations of individual SL9 fragmemts (Benner and McKinnon [1995]) suggest that the SL9 progenitor approached Jupiter by passing by L_1 or L_2 from a short-period heliocentric orbit between either Jupiter and Mars or between Jupiter and Saturn (Figure 2(a)). The distribution of heliocentric a and e determined from these fragment integrations are shown in Figure 2(b). The pre-collision fragments have Tisserand parameters of about $T = 3.02 \pm 0.01$. From this value and the similarity of the pre-collision orbits to the known QHs, Benner and McKinnon [1995] suggest a QH origin for SL9.

Twice as many fragments came from the outer asteroid belt as compared to the inner transjovian region. However, Benner and McKinnon [1995] do not conclude that SL9 originated from the outer asteroid belt. Instead, they say that "the chaos in SL9's orbit is so strong...that what is being seen is a statistical scrambling of all possible trajectories for an object as loosely bound as SL9." The bias toward as asteroid origin is a measure of the relative ease of capture (or escape) toward L_1 versus L_2, a known result (Heppenheimer and Porco [1977]). The statistical likelihood of a pre-collision interior orbit depends on the relative populations of interacting comets interior or exterior to Jupiter. If there are roughly equal populations, then a pre-collision interior origin is favored.

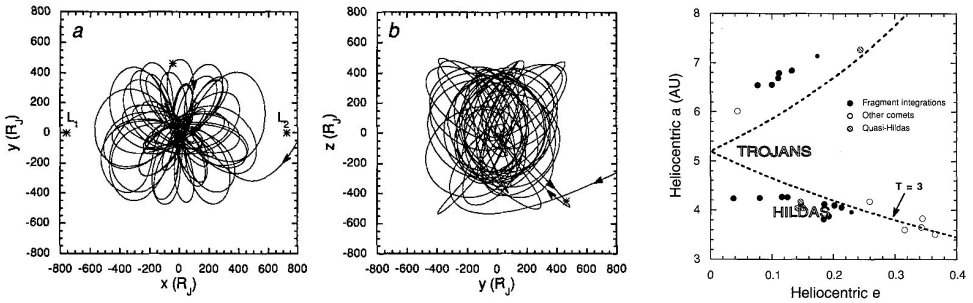

(a) (b)

Figure 2: (a) A typical SL9 trajectory showing the passage past a libration point and subsequent capture. The sun is to the right. (Reproduced from Benner and McKinnon [1995]. According to their terminology, their L_2 is our L_1, and vice versa.) (b) Heliocentric a and e of possible SL9 progenitor orbits, based on fragment integrations. The positions of selected comets and two major outer belt asteroid groups, the Trojans and the Hildas, are shown. The dashed curves are for Tisserand parameter $T = 3$ (for zero inclination); orbits above the upper curve and below the lower curve have $T > 3$ and are generally not Jupiter-crossing, while those between the two curves ($T < 3$) are Jupiter-crossing. (Reproduced from Benner and McKinnon [1995].)

2 Transport in the Planar Circular Restricted Three-Body Problem

When the dynamics are chaotic, statistical methods may be appropriate (Wiggins [1992]). By following ensembles of phase space trajectories, we can determine transition probabilities concerning how likely particles are to move from one region to another.

Following Wiggins [1992], suppose we study the motion on a manifold $\mathcal{M}$. Further, suppose $\mathcal{M}$ is partitioned into disjoint regions

$$R_i, i = 1, \ldots, N_R,$$

such that

$$\mathcal{M} = \bigcup_{i=1}^{N_R} R_i.$$

At $t = 0$, region R_i is *uniformly covered* with species S_i. Thus, species type of a point indicates the region in which it was located initially.

The statement of the transport problem is then as follows:

> *Describe the distribution of species $S_i, i = 1, \ldots, N_R$, throughout the regions $R_j, j = 1, \ldots, N_R$, for any time $t > 0$.*

Some quantities we would like to compute are: $T_{i,j}(t)$, the amount of species S_i contained in region R_j, and $F_{i,j}(t) = \frac{dT_{i,j}}{dt}(t)$, the flux of species S_i into region R_j (see Figure 3). For some problems, the probability of transport between two regions or the probability of an event occurring (e.g., collision), may be more relevant.

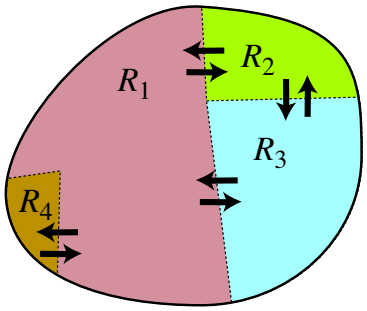

Figure 3: The manifold $\mathcal{M}$ is partitioned into the regions $R_i, i = 1, \ldots, N_R$. If points are distributed uniformly over $\mathcal{M}$ at $t = 0$, we want to compute the movement of points between these regions for all times $t > 0$.

Planar Circular Restricted Three-Body Problem. Here we only review the material concerning the PCR3BP which has relevance toward our discussion of transport. See details in Szebehely [1967] and Koon, Lo, Marsden, and Ross [2001].

Consider motion in the standard rotating coordinate system as shown in Figure 4 with the origin at the center of mass, and the sun and Jupiter fixed on the x-axis at the points $(-\mu, 0)$ and $(1-\mu, 0)$ respectively. Let (x, y) be the position of the comet in the plane, then the equations of motion in this rotating frame are:

$$\begin{aligned} \ddot{x} - 2\dot{y} &= -U_x^{\text{eff}}, \\ \ddot{y} + 2\dot{x} &= -U_y^{\text{eff}}, \end{aligned}$$

where

$$U^{\text{eff}} = -\frac{1}{2}(x^2 + y^2) - \frac{1-\mu}{r_1} - \frac{\mu}{r_2}$$

is the effective potential and the subscripts denote its partial derivatives and r_1, r_2 are the distances from the comet to the sun and the Jupiter respectively.

These equations are autonomous and can be put into Hamiltonian form. They have an energy integral:

$$E = \frac{1}{2}(\dot{x}^2 + \dot{y}^2) + U^{\text{eff}}(x, y).$$

which is related to the Jacobi integral C by $C = -2E$. The Jacobi integral can be expressed approximately in terms of the comet's semimajor axis, a, and eccentricity, e, in a form known as the Tisserand parameter, T, i.e., $C = T + \mathcal{O}(\mu)$, where

$$T = \frac{1}{a} + 2\sqrt{a(1-e^2)}.$$

The energy manifolds,

$$\mathcal{M}(\mu, \varepsilon) = \{(x, y, \dot{x}, \dot{y}) \mid E(x, y, \dot{x}, \dot{y}) = \varepsilon\}$$

where ε is a constant are 3-dimensional surfaces foliating the 4-dimensional phase space. For fixed μ and ε, the Hill's region is the projection of the energy manifold onto the position space

$$M(\mu, \varepsilon) = \{(x, y) \mid U^{\text{eff}}(x, y) \leq \varepsilon\},$$

and is the region in the xy-plane where the comet is energetically permitted to move The forbidden region is the region which is not accessible for the given energy. See Figure 4(b).

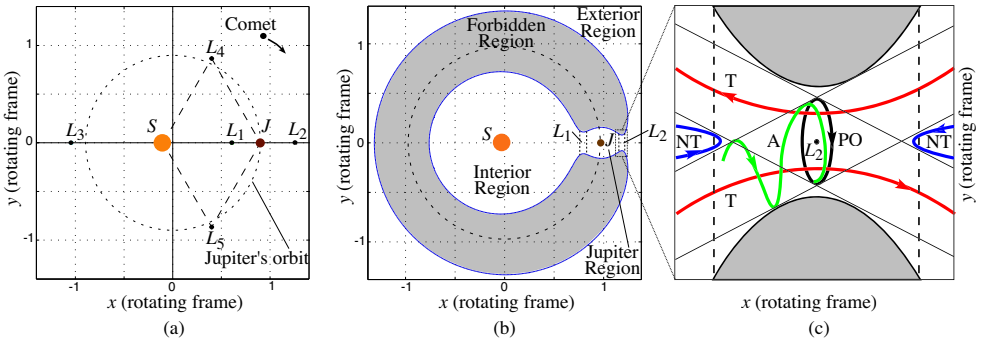

Figure 4: (a) The rotating frame showing the libration points, in particular L_1 and L_2, of the planar, circular restricted three-body problem. (b) Energetically forbidden region is gray "C". The Hill's region, $M(\mu, \varepsilon)$ (region in white), contains a bottleneck about L_1 and L_2. (c) The flow in the region near L_2, showing a periodic orbit around L_2 (labeled PO), a typical asymptotic orbit winding onto the periodic orbit (A), two transit orbits (T) and two non-transit orbits (NT). A similar figure holds for the region around L_1.

Eigenvalues of the linearized equations at L_1 and L_2 have one real and one imaginary pair, having a saddle $\times$ center structure. Our main concern is the behavior of orbits whose energy is just above that of L_2, for which the Hill's region is a connected region with an *interior* region (inside Jupiter's orbit), *exterior* region (outside Jupiter's orbit), and a *Jupiter* region (bubble surrounding Jupiter). We will use the terminology interior, exterior, and Jupiter regions to mean regions in the Hill's region and the corresponding regions of the energy surface, $\mathcal{M}(\mu, \varepsilon)$. Thus, we have a useful partition for our problem for which we can compute transport properties. These regions are connected by bottlenecks about L_1 and L_2 and the comet can pass between the regions only through these bottlenecks. Inside each bottleneck, adjacent regions of the (e.g., the interior and Jupiter regions) share a common boundary in the energy surface. This common boundary is known as the transition state and has been used previously in astrodynamical transport calculations (Jaffé, Ross, Lo, Marsden, Farrelly, and Uzer [2002]). For our analysis of transport, we must focus on the bottlenecks.

In each bottleneck (one around L_1 and one around L_2), there exist 4 types of orbits, as given in Conley [1968] and illustrated in Figure 4(c): (1) an unstable *periodic* Lyapunov orbit; (2) four cylinders of *asymptotic* orbits that wind onto or off this period orbit, which form pieces of stable and unstable manifolds; (3) *transit* orbits which the comet must use to make a transition from one region to the other; and (4) *nontransit* orbits where the comet bounces back to its original region.

McGehee [1969] was the first to observe that the asymptotic orbits are pieces of the 2-dimensional stable and unstable invariant manifold tubes associated to the Lyapunov orbit and that they form the boundary between transit and nontransit orbits. The transit orbits, passing from one region to another, are those inside the cylindrical manifold tube. The nontransit orbits,

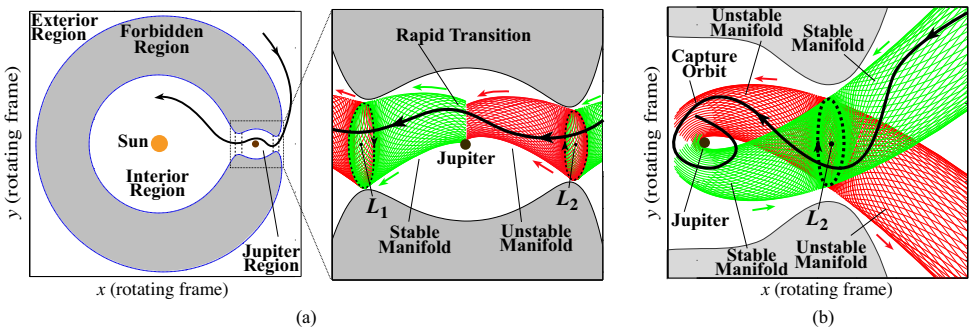

Figure 5: (a) An example of an interior-exterior transit orbit. This on goes from outside to inside Jupiter's orbit, passing by Jupiter. The tubes containing transit orbits—bounded by the cylindrical stable (lightly shaded) and unstable (darkly shaded) manifolds—intersect such that a transition is possible. (b) An orbit beginning inside the stable manifold tube in the exterior region is temporarily captured by Jupiter. When the tubes intersect the surface of Jupiter, a collision is possible.

which bounce back to their region of origin, are those outside the tube. Most importantly, to transit from outside Jupiter's orbit to inside (or vice versa), or get temporarily captured, a comet *must* be inside a tube of transit orbits, as in Figures 5(a) and 5(b). The invariant manifold tubes are global objects—they extend far beyond the vicinity of the bottleneck, partitioning the energy manifold.

Numerical Computation of Invariant Manifolds. Key to our analysis is the computation of the invariant manifolds of Lyapunov orbits, thus we include some notes on computation methods. Periodic Lyapunov orbits can be computed using a high order analytic expansion (see Llibre, Martinez, and Simó [1985]) or by using continuation methods (Doedel, Paffenroth, Keller, Dichmann, Galan, and Vanderbauwhede [2002]). Their stable and unstable manifolds can be approximated as given in Parker and Chua [1989]. The basic idea is to linearize the equations of motion about the periodic orbit and then use the monodromy matrix provided by Floquet theory to generate a linear approximation of the stable manifold associated with the periodic orbit. The linear approximation, in the form of a state vector, is numerically integrated in the nonlinear equations of motion to produce the approximation of the stable manifold. All numerical integrations were performed with a standard seventh-eighth order Runge-Kutta method.

Interior-Exterior Transition Mechanism. The heart of the transition mechanism from outside to inside Jupiter's orbit (or vice versa) is the intersection of tubes containing transit orbits. We can see the intersection clearly on a 2-dimensional Poincaré surface-of-section in the 3-dimensional energy manifold. We take our surface to be $\Sigma_{(\mu,\varepsilon)} = \{(y, \dot{y}) | x = 1 - \mu, \dot{x} < 0\}$, along a vertical line passing through Jupiter's center as in Figure 6(a). In Figure 6(b), we plot $\dot{y}$ versus y along this line, we see that the tube cross-sections are distorted circles. Upon magnification in Figure 6(c), it is clear that the tubes indeed intersect.

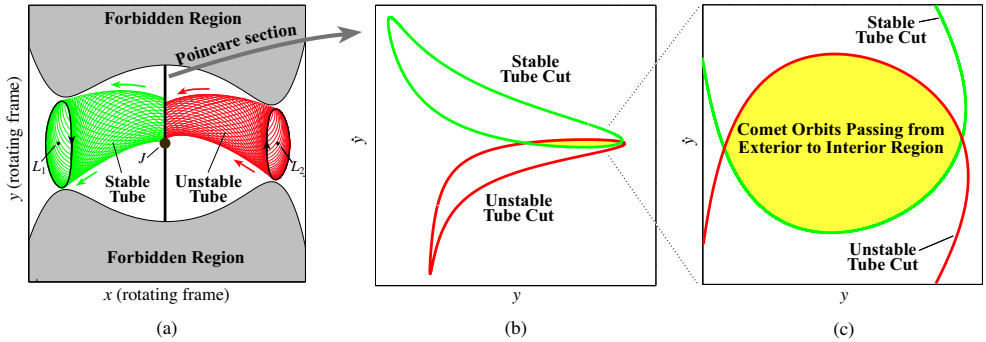

Figure 6: (a) We take a Poincaré surface-of-section $\Sigma_{(\mu,\varepsilon)} = \{(y, \dot{y}) | x = 1-\mu, \dot{x} < 0\}$, along a vertical line through the center of Jupiter (J). Both the L_1 and L_2 periodic orbit invariant manifold tubes intersect $\Sigma_{(\mu,\varepsilon)}$ transversally. (b) On $\Sigma_{(\mu,\varepsilon)}$, we see the first unstable tube cut for L_2 and first stable tube cut for L_1. (c) A small portion of the interior of the tubes intersect—this set in the energy manifold $\mathcal{M}(\mu, \varepsilon)$ containing the comet orbits which pass from the exterior to the interior region.

Any point within the region bounded by the curve corresponding to the stable tube cut is on an orbit that will go from the Jupiter region into the interior region. Similarly, a point within the unstable tube cut is on an orbit that came from the exterior region into the Jupiter region. A point inside the region bounded by the intersection of both curves (lightly shaded in Figure 6(c)) is on an orbit that makes the transition from the exterior region to the interior region, via the Jupiter region.

Interior-Exterior Transition Probability. Note that since $p_y = \dot{y} + x$ and x is constant, the $(y, \dot{y})$ plane is a linear displacement of the canonical plane (y, p_y). Furthermore, the action integral around any closed loop Γ on $\Sigma_{(\mu,\varepsilon)}$,

$$S = \oint_\Gamma p \cdot dq = \oint p_y \, dy,$$

is simply the area enclosed by Γ on the surface-of-section $\Sigma_{(\mu,\varepsilon)}$ (Meiss [1992]).

The agreement between a Monte-Carlo simulation and a Markov approximation in an earlier paper (Jaffé, Ross, Lo, Marsden, Farrelly, and Uzer [2002]) suggests that for energies slightly above L_1 and L_2, there are components of the energy surface for which the motion is "well mixed" (cf. Meiss [1992]). Thus, the Markov approximation is a good one. Let R_1 be the interior region and R_2 be the exterior region. In the Markov approximation, the probability of a particle going from region R_i to R_j is

$$P_{ij} = \frac{\mathcal{F}_{ij}}{A_j}$$

where A_j is the area of the first unstable tube cut on $\Sigma_{(\mu,\varepsilon)}$, containing transit orbits from R_j, and $\mathcal{F}_{ij} = \mathcal{F}_{ji}$ is the area of overlap of the first unstable tube cut from R_j and the first stable tube cut from R_i on $\Sigma_{(\mu,\varepsilon)}$. This transition probability is exact for one iterate of the Poincaré map; however, it is typically only qualitatively correct for longer times.

In Figure 7, we give the results of the calculations of P_{12} and P_{21} for mass paramter $\mu = 9.537 \times 10^{-4}$ and a variety of energies in the range of QH Jupiter-family comets. This is the probability of a comet to move from the interior to the exterior and vice versa during its first pass through the surface-of-section $\Sigma_{(\mu,\varepsilon)}$.

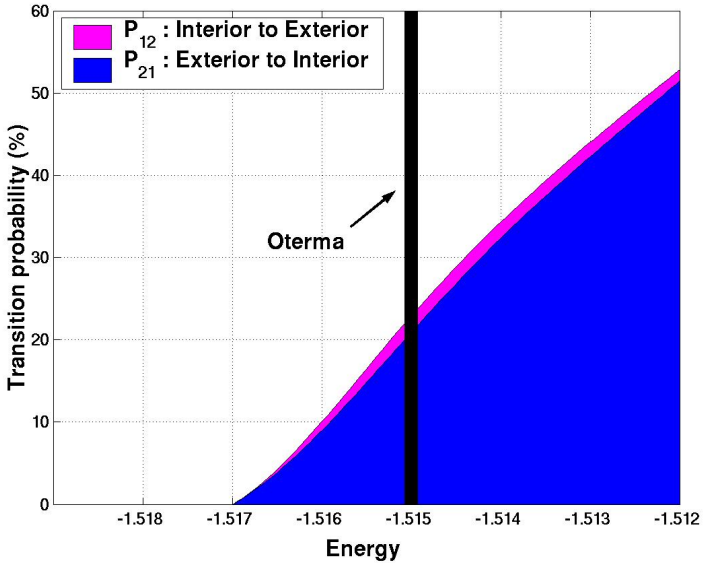

Figure 7: **Interior-exterior transition probabilities for quasi-Hilda Jupiter-family comets.** The probability of a comet to move from the interior to the exterior and vice versa during its first pass through the surface-of-section $\Sigma_{(\mu,\varepsilon)}$ is plotted as a function of energy in the planar, circular restricted three-body problem. The energy value of P/Oterma is shown for comparison. Note that interior to exterior transitions are slightly more probable than the reverse transition.

A few comments regarding this result are due. (1) Notice that there is a lower limit in energy, $E_t \approx -1.517$. For $E \leq E_t$, the tube cuts do not overlap and no direct transition is possible. After more loops around Jupiter, transition may be possible (cf. Koon, Lo, Marsden, and Ross [2000]). (2) The probability increases as a function of energy. (3) Quasi-Hilda P/Oterma is located in the region of $\approx 25\%$ probability. (4) Finally, notice that $P_{12} > P_{21}$, which is a result of $A_1 > A_2$, the slight asymmetry we shuld expect for a mass parameter of this value or larger (cf. Simó and Stuchi [2000]).

Collision Probabilities. Collision probabilities can be computed for objects coming through the L_1 and L_2 bottlenecks from the interior and exterior regions, respectively. We augment the procedure for computing interior-exterior transition probalities in the following way. Instead of computing $\mathcal{F}_{ij}$, we now compute the overlap of the first unstable manifold cut with the *diameter* of the secondary (e.g., Jupiter). Since the surface $\Sigma_{(\mu,\varepsilon)}$ passes through the center of secondary, any particle located on $\Sigma_{(\mu,\varepsilon)}$ with $|y| \leq R$ will have collided with the secondary, where R is the radius of secondary in units of the primary-secondary distance. This is illustrated in Figure 8.

There is a singularity at the center of the secondary, $y = 0$ on $\Sigma_{(\mu,\varepsilon)}$, so

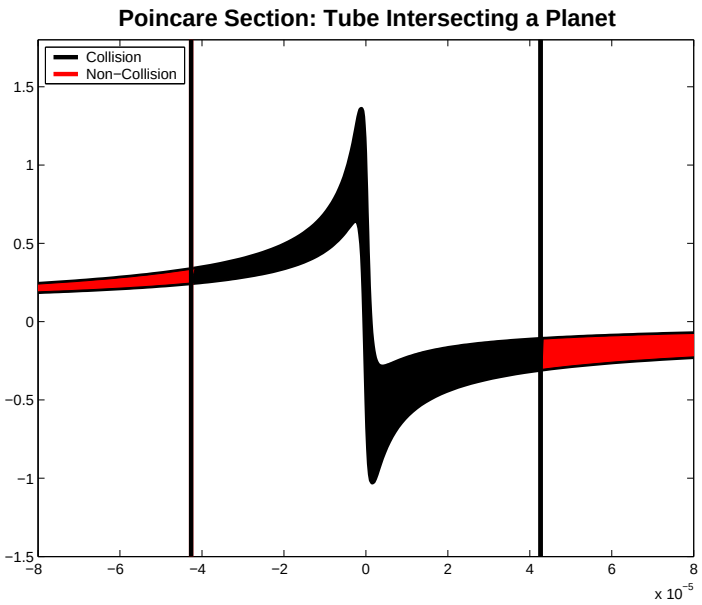

Figure 8: The surface-of-section, $\Sigma_{(\mu,\varepsilon)}$, is shown, with y vs. $\dot{y}$. The area inside the first unstable manifold tube cut with $|y| \leq R$ is shown in in black. These are orbits that collide with the surface of the secondary. The two vertical lines are at $y = \pm R$.

the calculation is actually performed along a nearby parallel surface-of-section, where $x = 1 - \mu \pm c$, with c a small number on the order of the integration tolerance (the '+' sign is for orbits coming from the exterior, and the '−' for orbits coming from the interior).

Collision probabilities for the sun-Jupiter case ($\mu = 9.537 \times 10^{-4}$, $R = 8.982 \times 10^{-5}$) are given in Figure 9. We notice the following. (1) The probability is not monotonically increasing as in Figure 7. (2) The energy range of possible pre-collision Shoemaker-Levy 9 orbits (from Benner and McKinnon [1995]) lies in the range of highest collision probability, suggesting the utility of this approach. (3) There is an asymmetry in orbits coming from the interior or the exterior, and now there are two lower energy cutoffs, $E_c^1 \approx -1.5173$ and $E_c^2 \approx -1.5165$, below which no collision can occur on the first pass by Jupiter. The asymmetry may be too slight to differentiate an interior origin from an exterior origin for SL9.

As a final computation, we address the NEA collision problem. For a mass parameter corresponding to the sun-Earth-asteroid problem ($\mu = 3.059 \times 10^{-6}$, $R = 4.258 \times 10^{-5}$), we compute the collision probability. The result is shown in Figure 10. It is interesting that the collision probabilities are nearly twice those for the quasi-Hilda case, even though Jupiter has a much larger mass and radius than the Earth. The asymmetry in interior/exterior originating orbits is not as pronounced as in Figure 9, owing to the smaller value of μ, and $E_c^1 \approx E_c^2 \approx -1.5 - 4.03 \times 10^{-4}$.

Conclusions

We address some questions regarding nonlinear comet and asteroid behavior by applying statistical methods to the planar, circular restricted three-body

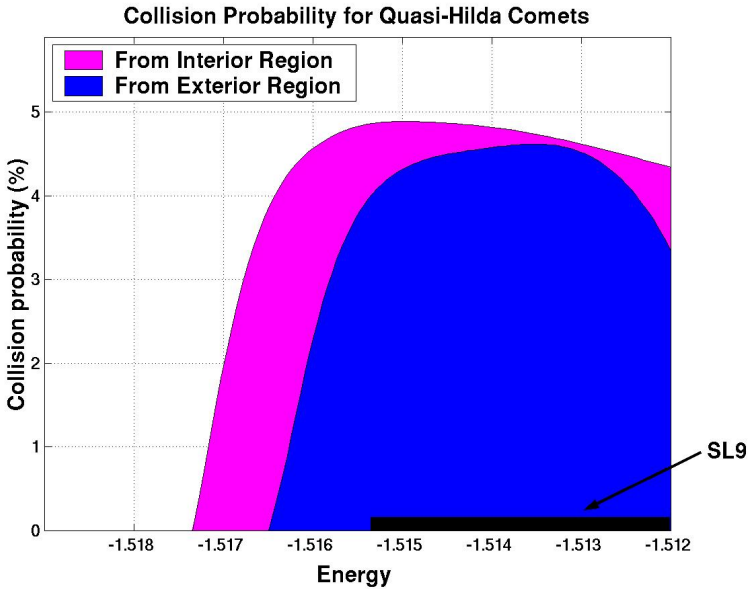

Figure 9: **Collision probabilities for quasi-Hilda comets.** The probability of collision for orbits making their first pass through the surface-of-section $\Sigma_{(\mu,\varepsilon)}$ is plotted as a function of energy. The energy range of possible pre-collision D/Shoemaker-Levy 9 orbits is shown for comparison.

problem. In particular, we make a Markov assumption regarding the phase space and compute probabilities of interior-exterior transition and collision with the secondary. Theory and observation are seen to agree for the comets P/Oterma and D/Shoemaker-Levy 9.

References

1. Belbruno, E. and B. Marsden [1997], Resonance hopping in comets. *The Astronomical Journal* **113**(4), 1433–1444.

2. Benner, L.A.M., and W.B. McKinnon [1995], On the orbital evolution and origin of comet Shoemaker-Levy 9. *Icarus* **118**, 155–168.

3. Carusi, A., L. Kresák, E. Pozzi, and G.B. Valsecchi [1985], *Long term evolution of short period comets.* Adam Hilger, Bristol, UK.

4. Chodas, P.W. and D.K. Yeomans [1993], The upcoming collision of comet Shoemaker-Levy 9 with Jupiter. *Bull. Am. Astron. Soc.* **25**.

5. Conley, C. [1968], Low energy transit orbits in the restricted three-body problem. *SIAM J. Appl. Math.* **16**, 732–746.

6. Doedel, E.J., R.C. Paffenroth, H.B. Keller, D.J. Dichmann, J. Galan, and A. Vanderbauwhede [2002], Continuation of periodic solutions in conservative systems with application to the 3-body problem. *Int. J. Bifurcation and Chaos.*, to appear.

7. Heppenheimer, T.A., and C. Porco [1977], New contributions to the problem of capture. *Icarus* **30**, 385–401.

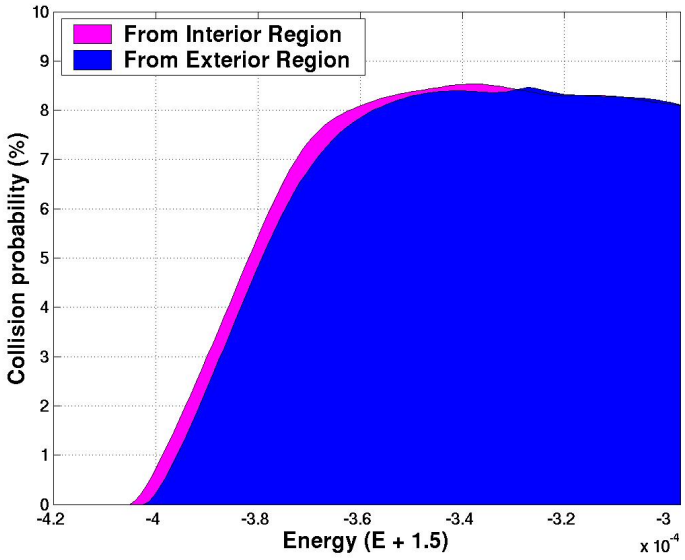

Figure 10: **Collision probabilities for near-Earth asteroids.** Note that the collision probabilities are nearly twice those for the quasi-Hilda case in Figure 9, even though Jupiter has a much larger mass and radius than the Earth.

8. Howell, K.C., B.G. Marchand, and M.W. Lo [2000], Temporary satellite capture of short period Jupiter family comets from the perspective of dynamical systems. *AAS/AIAA Space Flight Mechanics Meeting, Clearwater, Florida, USA. AAS Paper 00-155.*

9. Jaffé, C., S.D. Ross, M.W. Lo, J. Marsden, D. Farrelly, and T. Uzer [2002], Statistical theory of asteroid escape rates, *Physical Review Letters* **89**, 011101.

10. Kary, D.M., and L. Dones [1996], Capture statistics of short-period comets: implications for comet D/Shoemaker-Levy 9. *Icarus* **121**, 207–224.

11. Koon, W.S., M.W. Lo, J.E. Marsden, and S.D. Ross [2000], Heteroclinic connections between periodic orbits and resonance transitions in celestial mechanics. *Chaos* **10**(2), 427–469.

12. Koon, W.S., M.W. Lo, J.E. Marsden, and S.D. Ross [2001], Resonance and capture of Jupiter comets. *Celestial Mechanics and Dynamical Astronomy* **81**(1-2), 27–38.

13. Kresák, L. [1979], Dynamical interrelations among comets and asteroids. In *Asteroids* (T. Gehrels, Ed.), pp. 289–309. Univ. of Arizona Press, Tucson.

14. Gómez, G., W.S. Koon, M.W. Lo, J.E. Marsden, J. Masdemont, and S.D. Ross [2001], Invariant manifolds, the spatial three-body problem and space mission design. *AAS/AIAA Astrodynamics Specialist Conference, Quebec City, Canada, Aug. 2001.*

15. Llibre, J., R. Martinez, and C. Simó [1985] Transversality of the invariant manifolds associated to the Lyapunov family of periodic orbits near L2 in the restricted three-body problem. *Journal of Differential Equations* **58** 104–156.

16. Lo, M.W. and S.D. Ross [1997], Surfing the interplanetary tides. *Bull. Am. Astron. Soc.* **29**(3), 1021.

17. Marsden, B.G. [1993], *IAU Circ.* 5726.

18. McGehee, R. [1969], Some homoclinic orbits for the restricted three body problem. *Ph.D. Thesis*, University of Wisconsin, Madison, Wisconsin, USA.

19. Meiss, J.D. [1992], Symplective maps, variational principles, and transport. *Reviews of Modern Physics* **64**(3), 795–848.

20. Parker, T.S. and L.O. Chua [1989], *Practical numerical algorithms for chaotic systems*, Springer-Verlag, New York.

21. Simó, C., and T.J. Stuchi [2000], Central stable/unstable manifolds and the destruction of KAM tori in the planar Hill problem. *Physica D* **140**(1-2), 1–32.

22. Szebehely, V. [1967], *Theory of orbits*, Academic Press, New York.

23. Tancredi, G., M. Lindgren, and H. Rickman [1990], Temporary satellite capture and orbital evolution of comet P/Helin-Roman-Crockett. *Astronomy and Astrophysics* **239**, 375–380.

24. Valsecchi, G.B. [1992], Close encounters, planetary masses, and the evolution of cometary orbits. In *Periodic Comets* (J.A. Fernández and H. Rickman, Eds.), pp. 143–157. Univ. de la Republica, Montevideo, Uruguay.

25. Wiggins, S. [1992] *Chaotic transport in dynamical systems.* Interdisciplinary Appl. Math. **2**, Springer-Verlag, New York.